

Preparation of Atomically Flat Si(111)-H Surfaces in Aqueous Ammonium Fluoride Solutions Investigated by Using Electrochemical, *In Situ* EC-STM and ATR-FTIR Spectroscopic Methods

Sang-Eun Bae, Mi-Kyung Oh, Nam-Ki Min, Se-Hwan Paek, Suk-In Hong, and Chi-Woo J. Lee*

College of Science and Technology, Korea University, Jochiwon, Choongnam 339-704, Korea

Received July 6, 2004

Electrochemical, *in situ* electrochemical scanning tunneling microscope (EC-STM), and attenuated total reflectance-FTIR (ATR-FTIR) spectroscopic methods were employed to investigate the preparation of atomically flat Si(111)-H surface in ammonium fluoride solutions. Electrochemical properties of atomically flat Si(111)-H surface were characterized by anodic oxidation and cathodic hydrogen evolution with the open circuit potential (OCP) of *ca.* -0.4 V in concentrated ammonium fluoride solutions. As soon as the natural oxide-covered Si(111) electrode was immersed in fluoride solutions, OCP quickly shifted to near -1 V, which was more negative than the flat band potential of silicon surface, indicating that the surface silicon oxide had to be dissolved into the solution. OCP changed to become less negative as the oxide layer was being removed from the silicon surface. *In situ* EC-STM data showed that the surface was changed from the initial oxide-covered silicon to atomically rough hydrogen-terminated surface and then to atomically flat hydrogen-terminated surface as the OCP moved toward less negative potentials. The atomically flat Si(111)-H structure was confirmed by *in situ* EC-STM and ATR-FTIR data. The dependence of atomically flat Si(111)-H terrace on mis-cut angle was investigated by STM, and the results agreed with those anticipated by calculation. Further, the stability of Si(111)-H was checked by STM in ambient laboratory conditions.

Key Words : Si(III)-H, EC-STM, ATR-FTIR, Ammonium fluoride, Electrochemistry

Introduction

Since Higashi *et al.* reported that basic solutions produced ideally terminated Si(111) surfaces with silicon monohydride oriented normal to the surface with low defect density,¹ Si(111)-H surface has been a model surface for silicon research in finding an alternative cleansing solution.² As the length scales of silicon fabrication approach atomic dimensions,^{3,4} it has also been a model surface in researching nano structures.

The traditional cleaning process of silicon wafers is composed of several steps: degreasing, stripping of metal, silicon oxide forming, and stripping of the oxide layer. In this process, the last step performed in the acidic fluoride solutions forms hydrogen bonds on silicon surface, which, however, leaves the surface atomically rough.⁵ In the case of Si(111) wafer, the treatments in neutral or basic fluoride solutions must follow subsequently to complete the atomically flat and hydrogen-terminated surfaces. The hydrogen termination of silicon surface in buffered fluoride solution plays the most important role in producing high quality surface of the silicon.

Following the report on Si(111)-H treated in buffered solutions,¹ Higashi *et al.* have performed a large number of FTIR studies for pH dependence and chemical structures of the Si(111)-H surface.⁶ Pietsch *et al.* reported on the *ex situ* STM results of Si/SiO₂ interface obtained in concentrated

HF solution, which composed of small islands and pits with atomic roughness.⁷ More detailed results of the preparation of atomically flat Si(111)-H surface can be seen in Behm's work in which the appearance of Si(111) surface investigated by *ex situ* STM was drastically changed with immersion time in 40% NH₄F solution.⁸ As the immersion time increased, the islands and pits disappeared, and the flat terraces became wider. This is attributed to the step flow reaction of the Si(111)-H surface. Similar results were also observed in FTIR papers by Ito⁹ and Niwano.¹⁰ Recently, there is a growing tendency to skip the pretreatment process with the concentrated HF solution because in the 40% NH₄F solution, the ideally flat surface of Si(111)-H can be obtained by going through only one step.

Although the preparation of the atomically flat Si(111)-H surface is very important, structural changes occurring during the preparation procedures and the structural stability are little known. This work presents the results obtained by *in situ* electrochemical scanning tunneling microscope (EC-STM) and attenuated total reflectance-FTIR (ATR-FTIR) spectroscopic and electrochemical methods while the atomically flat Si(111)-H surface was prepared in aqueous fluoride solutions. We also report on the stability of ideally hydrogen-terminated Si(111) surfaces in ambient laboratory conditions.

Experimental Section

Silicon (111) wafers (n-type, 1-12 Ω cm, $<0.5^\circ$ mis-cut)

*Corresponding Author. e-mail: cwlee@korea.ac.kr

were cleaned in a sonication bath of milli-Q water (resistivity $> 18 \text{ M}\Omega\text{cm}$) and acetone, oxidized in a $\text{H}_2\text{O}_2 : \text{H}_2\text{SO}_4$ (1 : 1) solution for 20 min, rinsed with a milli-Q water, and finally dried in the flowing purified nitrogen gas.¹¹ The EC-STM experiment was carried out by using a PicoSPM and PicoStat (Molecular Imaging Corp.). Ohmic contact was made to the Si by GaIn alloy. Pt wire and loops were used as the reference electrode and the counter electrode, respectively. All potentials are quoted versus saturated calomel electrode (SCE) for convenience. EC-STM tips were prepared by electrochemical etching of a tungsten wire (0.25 mm in diameter) in 1 M NaOH solutions and followed by electrical insulating with Apiezon wax to minimize the faradaic current at the tip.¹²⁻¹⁴ All reactions and EC-STM scanings of silicon surface were conducted in an oxygen-free chamber at room temperature under the dark. All the chemicals used in this work were of the best quality available commercially and were used without further purification. Solutions were made of Milli-Q water.

Results and Discussion

Figure 1 shows a cyclic voltammogram (CV) of Si(111)-H surface in 40% NH_4F solution, scan rate = 50 mV/s after the preparation of atomically flat Si(111)-H. The potential was first swept negatively from the open circuit potential (-0.4 V) to -0.8 V . The cathodic current observed in the negative sweep is attributed to the evolution of hydrogen on the silicon surface.¹⁵ In the positive direction, the first shoulder current around -0.2 V was observed, and as the potential increased, the current increased and reached a flat region at $+0.2 \text{ V}$. It has been known that the current is attributed to the oxidation of Si-H bonds with the injection of an electron to the conduction band of the *n*-Si(111) electrode, forming dangling bonds of Si- and H^+ in solution. The surface dangling bond of Si is expected to be attacked further by either H_2O or F^- .^{15,16}

Figure 2 shows changes in open circuit potential (OCP)

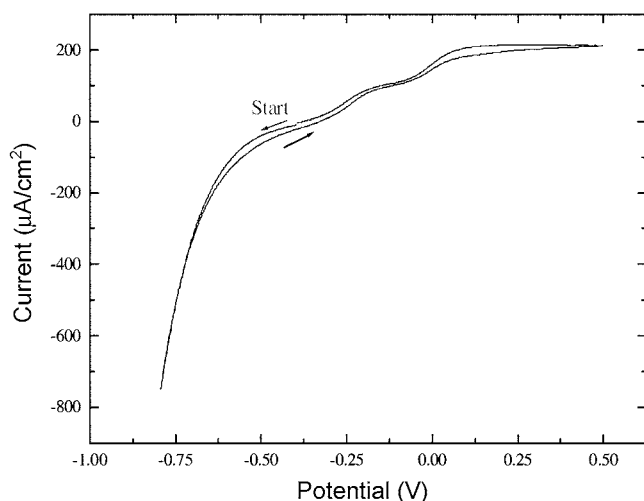


Figure 1. Cyclic voltammogram of Si(111)-H surface in 40% NH_4F solution, scan rate 50 mV/s.

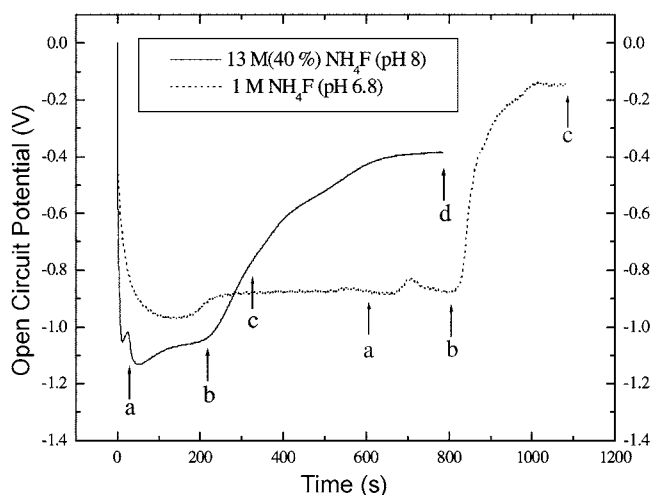


Figure 2. Open circuit potential shifts of Si(111) surfaces during the preparations of the Si(111)-H surfaces in 40% NH_4F solution at pH 8.0 and 1 M NH_4F solution at pH 6.8. The marks, a, b, c, and d, correspond to the points of EC-STM images in Figure 3 and Figure 4.

when Si(111) electrode covered with oxides was immersed in 40% NH_4F solution at pH 8.0 and in 1 M NH_4F solution at pH 6.8. The OCP can be deduced as being identified as a redox mixed potential, resulting from the current densities of positive and negative charge transfers, including both thermodynamic terms of silicon oxide removal and silicon oxidation by fluoride ion and of silicon reduction by proton and kinetic terms j_{OC} and j_{OA} , the exchange current densities for the anodic and cathodic processes.¹⁷ In Figure 2, both of the OCPs sharply decreased toward negative potential as soon as the silicon wafers were immersed in fluoride solutions, indicating that redox reactions on Si surfaces started simultaneously with the immersion of silicon wafer in fluoride solutions. After the OCP in 1 M NH_4F solution decreased until -0.95 V , a flat region and an abruptly positive shift of the OCP sequentially appeared. On the other hand, the OCP in 40% NH_4F solution showed two dips at (-1.05 V , 12 s) and at (-1.13 V , 50 s), increased gradually, and then increased rapidly with the rate slower than the one in 1 M NH_4F solution. In this situation, it is necessary to find out what kind of electrochemical redox species exists in the system. The surfaces of silicon wafer pretreated in piranha solution were fully covered with the thin silicon oxide layers, and there were fluoride ions, protons, water, and ammonium ions in the aqueous fluoride solutions. Thus, at the interface between silicon oxide and solution, dissolution reaction of the oxide layer and hydrogen evolution reaction took place as anodic and cathodic reactions, respectively. The initial OCPs were near -1.0 V , which is more negative potential than the flat band potential (-0.4 V)¹⁸ of the silicon, suggesting that electrochemical reactions were taking place mostly through anodic pathways, based on the model of silicon electrode in fluoride solutions.¹⁷ The region near -1 V and the positive shift of OCP indicate that the dissolution of the oxide layer was taking place mostly in the beginning and gradually decreased. The terminal OCP

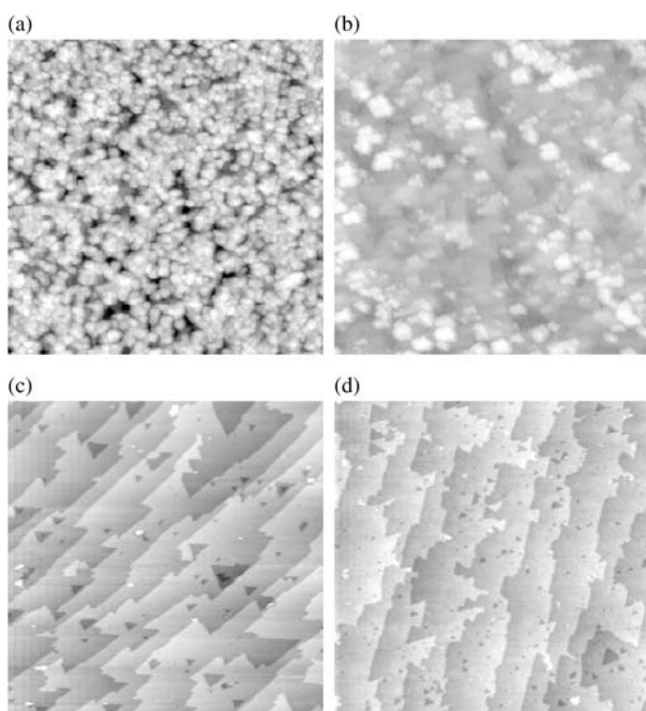


Figure 3. *In situ* EC-STM images ($500 \times 500 \text{ nm}^2$) of Si(111)-H surface obtained in 0.1 M sulfuric acid after etching silicon oxide in 1 M NH_4F solution at pH 6.8 for (a) 600 s, (b) 800 s, and (c) 1100 s. (d) was obtained after etching for 4600 s in 0.2 M NH_4F solution at pH 6.8.

values in the two different pH solutions were not equivalent, reflecting the difference in concentration and pH of the fluoride solutions. In general, it is accepted that the step flow reaction of Si(111)-H in acidic fluoride solution is slower than the one in basic solution.¹⁹ Therefore, at pH 8.0, step flow reactions take place predominantly more than at pH 6.8, which forces the OCP at pH 8.0 to be more negative than at pH 6.8. On the other hand, H^+ concentration in the solution may also contribute to the different value in OCP as much as expressed by the Nernst equation. EC-STM images were taken at different OCP values.

Figure 3 shows EC-STM images of Si(111) surfaces obtained in 0.1 M sulfuric acid after treatments of the thin oxide covered Si(111) samples for various times in 1 M NH_4F solution at pH 6.8. The first image (Fig. 3a) taken after etching in 1 M NH_4F solution at pH 6.8 for 600 s represents the side of silicon oxide surface with some native oxide layer removed. The height variation in the image shows the thickness of silicon oxide layer on silicon surfaces in which the heights of round silicon oxide range from 5 Å to 25 Å, which agrees very well with the reported thickness of silicon oxide layers.^{8,20} After the etching of the Si(111) surface for 800 s, the surface morphology was so changed (Fig. 3b). The round islands were still randomly distributed and the atomically flat surfaces and triangular pits appeared. After 1100 s etching in 1 M NH_4F solution, as shown in Figure 3c, the atomically flat surface of the Si(111)-H appeared wide. The typical feature of this surface is the perfect monohydrogen terminated terrace with about 3.1

bilayer step, which agrees well with the reported data.^{8,13,15,20} It has been known that pit free surface of the Si(111)-H is obtained in oxygen free 40% NH_4F solution.¹⁹ However, in this image, a few triangular pits are present that attributes to the pH difference with 40% NH_4F solution.²¹ The triangular pits inform that the sample was directional sliced Si(111) wafer which has the triangular pits pointed toward step direction and the straight steps. The mis-cut angle of Si(111) used in this work was below 0.5° , from which the observed terrace was in agreement with what was expected. Figure 3d represents the EC-STM image obtained after etching of Si(111)-H for 4600 s in 0.2 M fluoride solution at pH 6.8. The result shows that the reaction rate during the preparations of atomically flat Si(111)-H surface exhibits strong dependence on the fluoride ion concentration, because F^- ion is a major fluorine species in fluoride solution at pH 6.8.²¹

Figure 4 presents the *in situ* EC-STM images of Si(111) surface obtained after 30 s (a), 220 s (b), 320 s (c), and 800 s (d) etching in 40% NH_4F solution. After each immersion time, -0.3 V more than each OCP value was applied on Si(111) wafers to keep the morphology of the surface of each moment for EC-STM imaging. The sequentially obtained EC-STM images allow us to infer that the surface morphology did not change while approaching and engaging of the EC-STM tip at the potentials. Figure 4 shows a tendency similar to the Figure 3. But it is clear that there are differences between the two results. The first image (Fig. 4a) has a number of islands, extremely narrow flat surfaces, and pits. Figure 4b shows that the number of the islands decreased, and, in contrast, the flat surfaces became wider. In Figure 4c, most islands disappeared, and very flat surfaces were formed. But there were many kink steps and the triangular pits as in Figure 3c. In the next image Figure 4d, the kink steps and the triangular pits were disappeared to lead to the ideally flat terrace and the mono atomic step height of the Si(111)-H surface.

Now it is possible to compare the EC-STM results with the OCP changes. At the time near -1 V , the Si(111) surface consisted of the oxide layer, indicating that the dissolution reaction of silicon oxide dominated over the hydrogen evolution reaction. As the immersion time increased, the oxide layer of Si(111) surfaces were removed and, therefore, the reactants (silicon oxides) of the dissolution reaction decreased. This indicates that the OCP may change toward positive potential, which excellently agrees with the OCP results. The EC-STM results obtained in 40% NH_4F solution after being etched for 30 s indicate that most of the surface was covered with the silicon oxide layer, and that the flat terrace could not be observed and that instead rough surfaces were observed as shown in Figure 4a. From these results, one can deduce that the first dip at 12 s may reflect the breakage of oxide layer by attack of fluoride ions from solution.

The *in situ* EC-STM image of Figure 4b was obtained at the moment when the OCP started to increase abruptly (Fig. 2b). The image shows flat regions with some oxides left

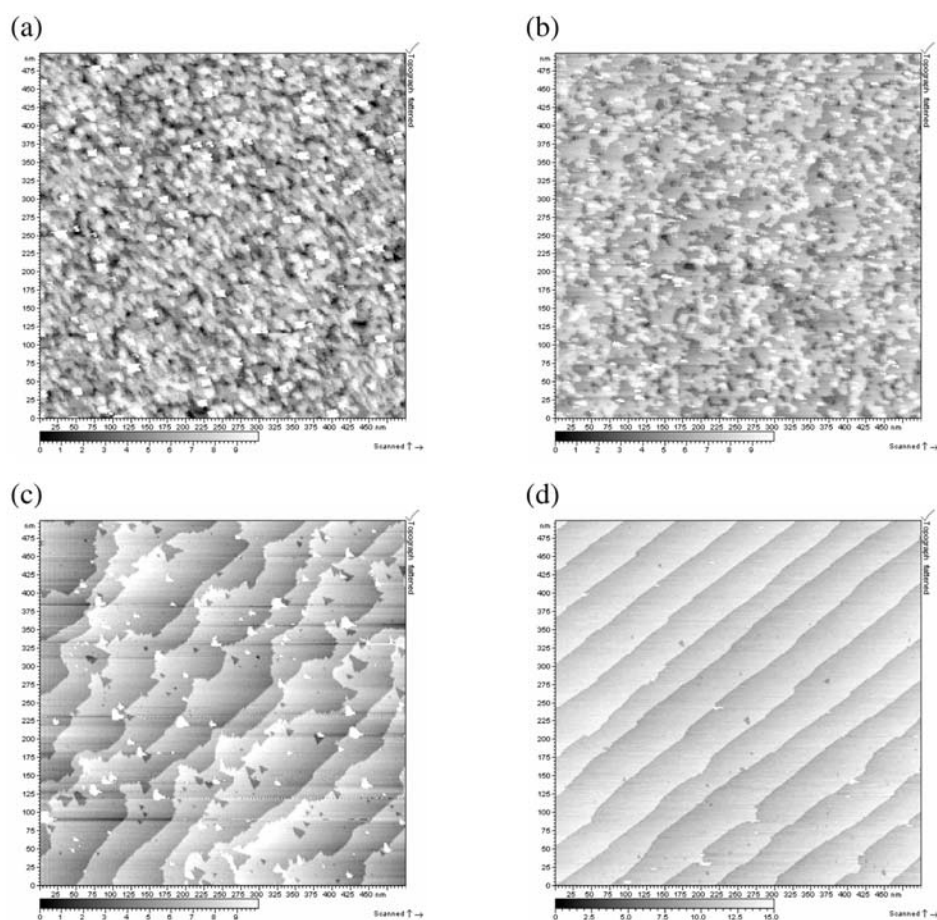


Figure 4. *In situ* EC-STM images ($500 \times 500 \text{ nm}^2$) of Si(111)-H surface during preparation of atomically flat Si(111)-H in 40% NH_4F solution. Immersion time: (a) 30 s, (b) 220 s, (c) 320 s, and (d) 800 s.

visible. The abrupt increase of the OCP was attributable to the significant disappearance of the oxide layer as a reactant of the oxidation reaction and to erosion of the unstable dihydrogen and trihydrogen terminated silicon to form the flat patches with mono-hydride covered. Thus, during the abruptly positive shift of the OCP, we can see that the unstable dihydrogen and trihydrogen terminated silicons were being removed. The second dip at 50 s may be related to the replacement of oxide surface to hydride.

Different concentrations of ammonium fluoride and proton were used in etching reactions to obtain Figure 3 and Figure 4. In general, the etching rate is known to be proportional to the concentration of fluoride and hydroxide although the exact functional form on etching reactions is still being debated.^{22,23} The oxide layer is believed to be removed more easily in acidic fluoride solutions than in basic solution.^{1,19} In contrast, the step flow reaction of the Si(111)-H surface, which is initiated by hydroxide ion, is known to be slower in acidic solution than in basic one.¹⁹ These facts are visualized in our EC-STM results. In 1 M NH_4F at pH 6.8, after the reactive dihydride and trihydride silicons were fast etched out, the surface leads to form terraces of straight sides of monohydride-terminated silicons with apexes of dihydride silicon atoms. Then, the etching reaction of Si(111)-H at the straight sides does not progress

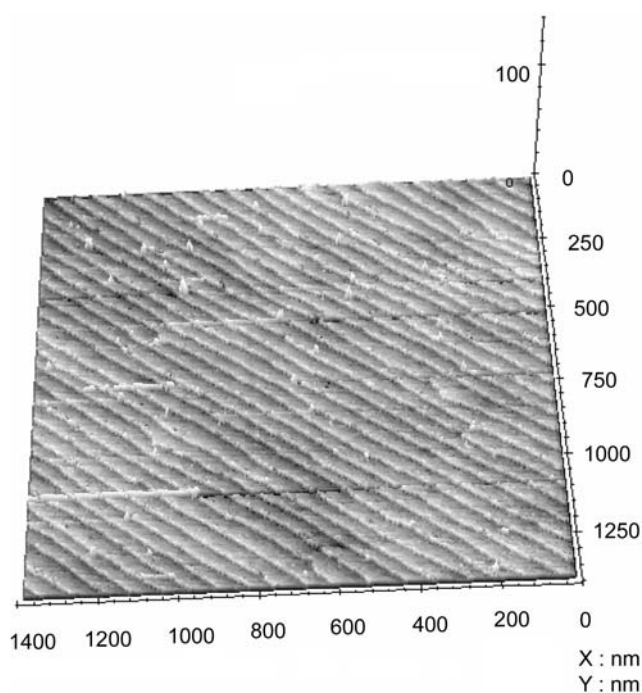


Figure 5. *In situ* EC-STM 3D image of Si(111)-H surface obtained after etching in 40% NH_4F solution for 800 s: $1400 \times 1400 \text{ nm}^2$. $V_{\text{tip}} = 0.0 \text{ V}$, $V_{\text{sample}} = -0.65 \text{ V}$, $I_t = 0.1 \text{ nA}$.

significantly and anodic current ceases to flow, which causes a very fast increase of OCP as shown in Figure 2. A minimum time to produce a flat surface, which was originated from the difference in the reaction rate between the kink site (apex of the triangular shape) reaction and the step flow initiation reaction, was *ca.* 1100 s in 1 M NH_4F at pH 6.8. In contrast, at pH 8.0 solution, the step flow reaction progress more rapidly because of more frequent attacks by relatively sufficient amount of hydroxide ions in the solution so that the apex of the triangular shape of the Si(111)-H surface could be fast eroded. A minimum time to produce a flat surface was 800 s in 40% NH_4F solution.

In summary, near -1 V region of the OCP, the stripping reaction of oxide dominated. On the other hand, at more

positive potentials that -1 V region, the step flow reaction was superior. As the OCP approached toward -0.4 V, the surface of Si(111)-H became ideally flat. As a result, the OCP can be a good parameter for the evaluation of Si(111) morphology during the preparation of the atomically flat Si(111)-H surface.

To show whether or not the EC-STM image taken locally represent an overall reaction on the Si(111)-H surface, we zoomed out *in situ* EC-STM image of the Si(111)-H surface. Figure 5 shows the 3-D image of the Si(111)-H surface with a larger area ($1400 \times 1400 \text{ nm}^2$) in the same solution of Figure 4, which supports that any region of the Si(111)-H surface shows the surface similar to the smaller area (Fig. 4d). The 3-D EC-STM image better describes the atomic stair case structure which is the typical feature of atomically flat Si(111)-H surface.

Figure 6 shows the morphology dependence on mis-cut angle of Si(111) wafer. STM images with 1000×1000 (a) and 300×300 (a') nm^2 areas of Si(111) sample with $\Delta\theta$ $3^\circ\sim 4^\circ$ mis-cut towards [11-2] after the preparation of Si(111)-H through the same procedures as above are presented in Figure 6a and 6a'. In Figure 6a, the steps and the terraces like those in Figure 3 and Figure 4 can not be seen. With the higher resolution (Fig. 6a'), the steps and terraces of 5 nm wide are distinguishable. This agrees well with the expectation. However, the surface in Figure 6 looks rougher than the ones in the Figure 3 and Figure 4, which can be attributed to the step pinning at the migrating step edges by some contaminants.¹⁹ The bulk defects are also observable in Figure 6a, which is supposed to be most likely the oxide cluster in the oxygen-containing Czochralski-grown silicon crystal.⁷ The Si(111) surfaces treated with the same procedures are also presented in Figure 6b and Figure 6c as 0.5 and 0.1 mis-cut samples, respectively, in which the terrace widths are consistent with the expected values as in Figure 6d.

Atomic resolution *in situ* EC-STM image obtained on the terrace of the Si(111)-H surface in 40% NH_4F solution is presented in Figure 7. The perfect hexagonal structure of the

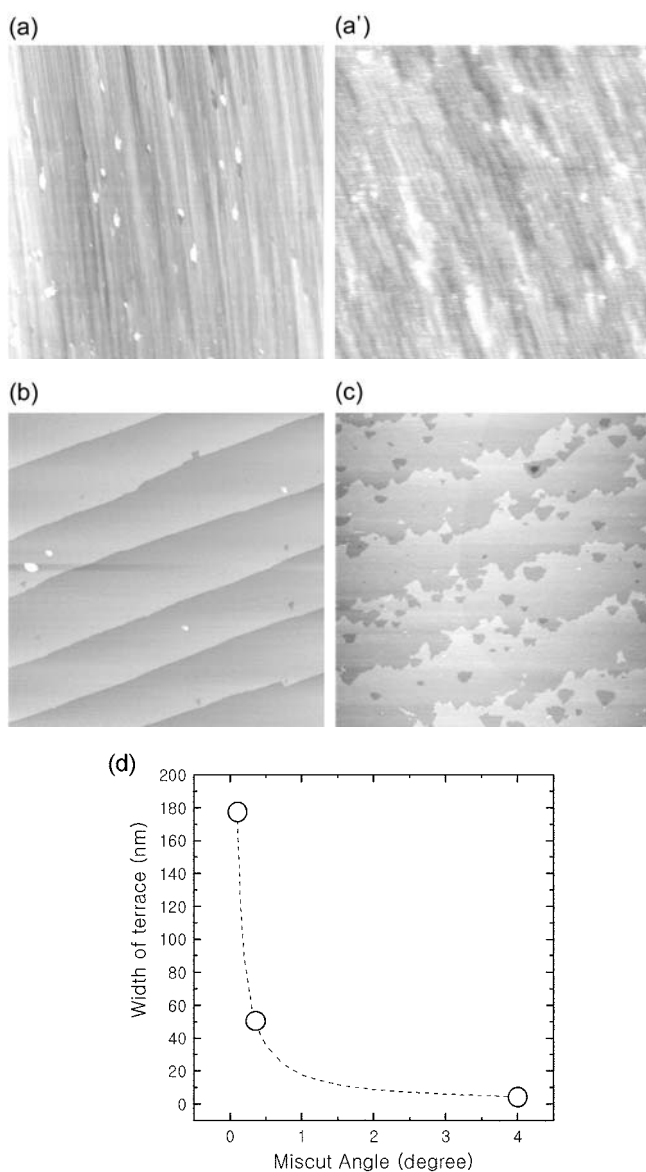


Figure 6. Terrace width as a function of Si(111) mis-cut angle. (a) $3\text{--}4^\circ$ ((a): $1000 \times 1000 \text{ nm}^2$ and (a') $300 \times 300 \text{ nm}^2$) (b) 0.35 ($300 \times 300 \text{ nm}^2$), and (c) 0.1 ($1000 \times 1000 \text{ nm}^2$). (d) The expected (dotted line) and experimental (open circle) terrace width as a function of Si(111) mis-cut angle.

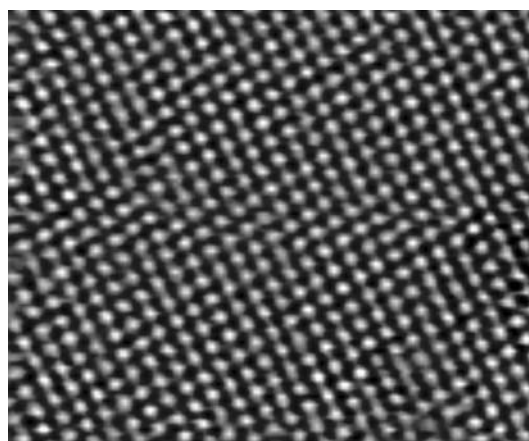


Figure 7. *In situ* atomic resolution EC-STM image ($9.76 \times 8.0 \text{ nm}^2$) of Si(111)-H surface in 40% NH_4F solution: $V_{\text{tip}} = 0.0$ V, $V_{\text{sample}} = -0.54$ V, $I_t = 1$ nA.

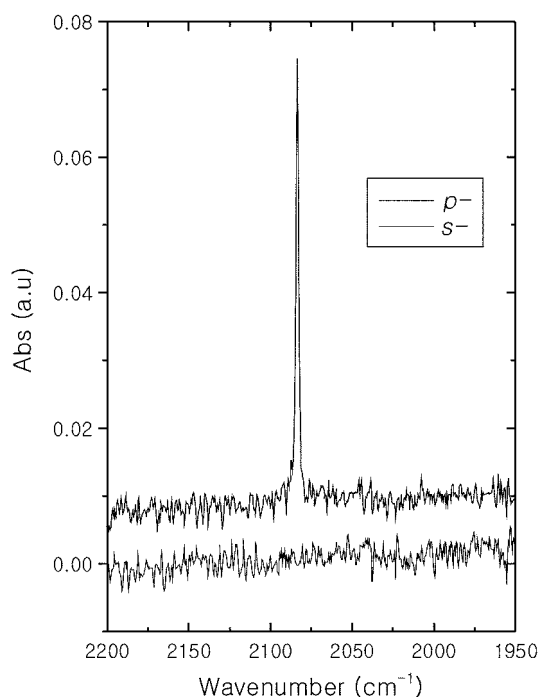


Figure 8. ATR FT-IR spectra of Si(111)-H surface after treatment of an oxidized Si(111) surface in 40% NH_4F solution.

Si(111) surface atoms with an interatomic distance of 3.8 Å was visible, indicating that the surface of Si(111)-H was ideally unreconstructed.²⁴ Each round spot corresponded to the upper silicon atom on Si(111) bilayer.

In order to analyze the chemical bond on silicon surface, ATR-FTIR experiments were performed. Figure 8 shows the ATR-FTIR spectra of the hydrogen-terminated Si(111) surface, which were measured under dry nitrogen environments with *p*- and *s*-polarization. The Si(111)-H sample was prepared following the same procedure as EC-STM samples. A sharp peak at 2083.7 cm^{-1} was observed in *p*-polarization mode only. This peak may be attributed to the Si-H stretching mode of the monohydride termination on the Si(111) surface, characterized by a polarization perpendicular to the surface.

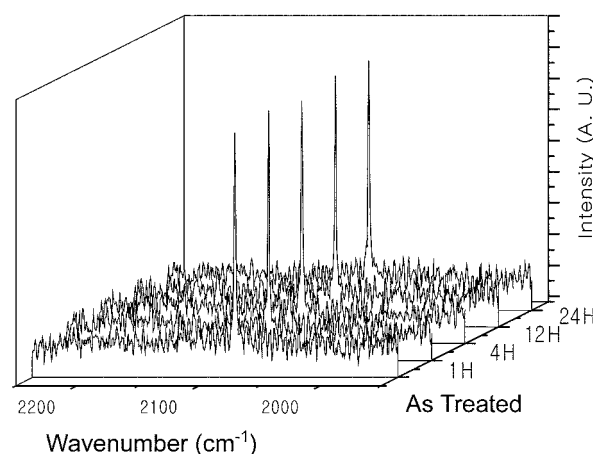


Figure 9. ATR-FTIR spectra of H-Si(111) surface in the region of 2250-1950 cm^{-1} after the sample was exposed to dry air for 0, 1 h, 4 h, 12 h, and 24 h.

ular to the surface. The result of the present study is in a good agreement with some previous reports.^{1,11,25,26,27} Thus from both ATR-FTIR and EC-STM results, one can see that hydrogen is mostly bound on the ideal (111) terrace as a monohydride.

Both the intensity and the full width at half maximum (FWHM) of the peak of the Si-H stretching on the H-Si(111) surface remained unchanged under dry air environments even after 24 hours or more as shown in Figure 9. In addition, no bands related to carbon contaminants were detected in the region of 2800-3000 cm^{-1} under the present experimental conditions, which means that the H-covered Si(111) surface was prepared carefully and was kept very stable.

The hydrogen terminated Si(111) surface is stable in dry air for several hours as previously mentioned. But the co-existence of oxygen and moisture in the atmosphere results in the oxidation of the Si(111)-H surface.²⁸ To see the stability of Si(111)-H in ambient laboratory conditions we probed Si(111)-H surfaces by STM. Figure 10 shows STM images obtained from as-prepared Si(111)-H sample (Fig.

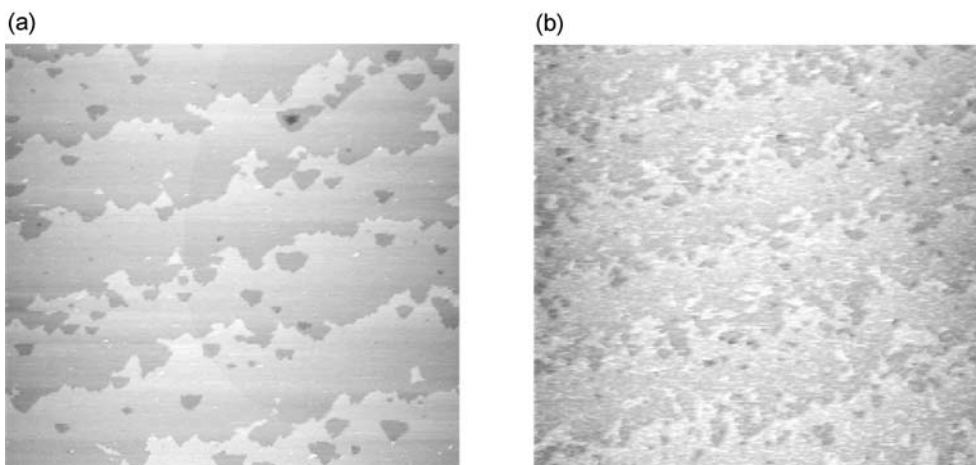


Figure 10. STM images ($1000 \times 1000 \text{ nm}^2$) of Si(111) surface before (a) and after (b) exposure to the air with 60% relative humidity for 13 hours.

10a) and the Si(111)-H sample left for 13 hours in the air with 60% relative humidity (Fig. 10b). The measurements were performed under Ar atmosphere after exposure to humid laboratory conditions. As shown in Figure 10b, although steps and terraces can be distinguishable, a large number of small spots with 2-3 Å height were produced, which is believed to be silicon oxide derived from the oxidation of silicon atoms by water and oxygen.²⁵ The results show that the prepared Si(111)-H sample should be stored either in water-free and/or in oxygen-free environmental conditions to keep the high quality of atomically smooth Si(111)-H surface and that the Si(111)-H exposed to the air of 60% relative humidity should be used with care so that the surface oxide spots formed do not interfere with further studies such as nano structure formation on the surface of Si(111)-H.

Conclusions

In situ EC-STM, OCP, ATR-FTIR, and CV measurements were employed to study the evolution of surface morphology during the preparation of atomically flat hydrogen terminated Si(111) surface. Atomically flat Si(111)-H surfaces were prepared very well not only in 40% NH₄F solutions but also in 1 M NH₄F solutions. This was confirmed by *in situ* EC-STM and ATR-FTIR results. The good (atomically flat) and poor (rough) quality of the Si(111)-H surface exhibited more positive and more negative open circuit potentials than the flat band potential of silicon, respectively, suggesting that the OCP can be a good parameter for the evaluation of flatness quality of the atomically flat Si(111)-H surface during the preparation of Si(111)-H.

Acknowledgements. Helpful discussions with Professors P. Allongue and J. Inukai are gratefully acknowledged. This work was supported by Korea Research Foundation (KRF-2002-070-C00050).

References

- Higashi, G. S.; Chabal, Y. J.; Trucks, G. W.; Raghavachari, K. *Appl. Phys. Lett.* **1990**, *56*, 656.
- Weldon, M. K.; Queeney, K. T.; Eng, J., Jr; Raghavachari, K.; Chabal, Y. J. *Surf. Sci.* **2002**, *500*, 859.
- Cai, W.; Lin, Z.; Strother, T.; Smith, L. M.; Hamers, R. J. *J. Phys. Chem. B* **2002**, *160*, 2656.
- Hurley, P. T.; Ribbe, A. E.; Buriak, J. M. *J. Am. Chem. Soc.* **2003**, *125*, 11334.
- Kern, W. *J. Electrochem. Soc.* **1990**, *137*, 1887.
- Jakob, P.; Chabal, Y. J. *J. Chem. Phys.* **1991**, *95*, 2897.
- Pietsch, G. J.; Kohler, U.; Henzler, M. *J. Appl. Phys.* **1993**, *73*, 4797.
- Houbertz, R.; Memert, U.; Behm, R. *J. Surf. Sci.* **1998**, *396*, 198.
- Nakamura, M.; Song, M.-B.; Ito, M. *Electrochim. Acta* **1996**, *41*, 681.
- Niwano, M.; Kondo, U.; Kimura, Y. *J. Electrochem. Soc.* **2000**, *147*, 1555.
- Lee, I.-C.; Bae, S.-E.; Song, M.-B.; Lee, J.-S.; Paek, S.-H.; Lee, C.-W. *J. Bull. Korean Chem. Soc.* **2004**, *25*, 167.
- Song, M.-B.; Jang, J.-M.; Lee, C.-W. *Bull. Korean Chem. Soc.* **2002**, *23*, 71.
- Bae, S.-E.; Lee, C.-W. J. Extended Abstracts of 205th ECS Meeting, 174, 2004.
- Woo, D.-H.; Yoo, J.-S.; Park, S.-M.; Jeon, I.-C.; Kang, H. *Bull. Korean Chem. Soc.* **2004**, *25*, 577.
- Kaji, K.; Yau, S.-L.; Itaya, K. *J. Appl. Phys.* **1995**, *78*, 5727.
- Gerischer, H.; Lubke, M. *Ber. Bunsenges. Phys. Chem.* **1987**, *91*, 394.
- Chelma, M.; Homma, T.; Bertagna, V.; Erre, R.; Kubo, N.; Osaka, T. *J. Electroanal. Chem.* **2003**, *559*, 111.
- Tomiat, E.; Matsuda, N.; Itaya, K. *J. Vac. Sci. Technol. A* **1990**, *8*, 534.
- Allongue, P.; Villeneuve, C. H. de; Morin, S.; Boukherroub, R.; Wayner, D. D. M. *Electrochim. Acta* **2000**, *45*, 4591.
- Yau, S.; Fan, F. F.; Bard, A. J. *J. Electrochem. Soc.* **1992**, *139*, 2825.
- Matsumura, M.; Fukidome, H. *J. Electrochem. Soc.* **1996**, *143*, 2683.
- Allongue, P.; KieLing, V.; Gerischer, H. *Electrochim. Acta* **1995**, *40*, 1353.
- Hines, M. A. *Int. Rev. Phys. Chem.* **2001**, *20*, 645.
- Kim, Y.; Lieber, C. M. *J. Am. Chem. Soc.* **1991**, *113*, 2333.
- Ye, S.; Ichihara, T.; Uosaki, K. *Appl. Phys. Lett.* **1999**, *75*, 1562.
- Ree, J.; Chang, K.; Kim, Y. H. *Bull. Korean Chem. Soc.* **2002**, *23*, 205.
- Ree, J.; Chang, K.; Kim, Y. H.; Shin, H. K. *Bull. Korean Chem. Soc.* **2003**, *24*, 986.
- Neuwald, U.; Hessel, H. E.; Feltz, A.; Memmert, U.; Behm, R. J. *Appl. Phys. Lett.* **1992**, *60*, 1307.